International Journal of Nanomedicine

Dovepress
open access to scientific and medical research

Open Access Full Text Article

ORIGINAL RESEARCH

Controlled release and angiotensin-converting enzyme inhibition properties of an antihypertensive drug based on a perindopril erbumine-layered double hydroxide nanocomposite

This article was published in the following Dove Press journal:
International Journal of Nanomedicine
20 April 2012
Number of times this article has been viewed

Samer Hasan Hussein Al Ali[1]
Mothanna Al-Qubaisi[2]
Mohd Zobir Hussein[1,3]
Maznah Ismail[2,4]
Zulkarnain Zainal[1]
Muhammad Nazrul Hakim[5]

[1]Department of Chemistry, Faculty of Science, [2]Laboratory of Molecular Biomedicine, Institute of Bioscience, [3]Advanced Materials and Nanotechnology Laboratory, Institute of Advanced Technology, [4]Department of Nutrition and Dietetics, Faculty of Medicine and Health Science, [5]Department of Biomedical Science, Faculty of Medicine and Health Science, Universiti Putra Malaysia, Serdang, Selangor, Malaysia

Background: The intercalation of perindopril erbumine into Zn/Al-NO_3-layered double hydroxide resulted in the formation of a host-guest type of material. By virtue of the ion-exchange properties of layered double hydroxide, perindopril erbumine was released in a sustained manner. Therefore, this intercalated material can be used as a controlled-release formulation.

Results: Perindopril was intercalated into the interlayers and formed a well ordered, layered organic-inorganic nanocomposite. The basal spacing of the products was expanded to 21.7 Å and 19.9 Å by the ion-exchange and coprecipitation methods, respectively, in a bilayer and a monolayer arrangement, respectively. The release of perindopril from the nanocomposite synthesized by the coprecipitation method was slower than that of its counterpart synthesized by the ion-exchange method. The rate of release was governed by pseudo-second order kinetics. An in vitro antihypertensive assay showed that the intercalation process results in effectiveness similar to that of the antihypertensive properties of perindopril.

Conclusion: Intercalated perindopril showed better thermal stability than its free counterpart. The resulting material showed sustained-release properties and can therefore be used as a controlled-release formulation.

Keywords: perindopril erbumine, layered double hydroxides, ion-exchange, coprecipitation, sustained release, angiotensin-converting enzyme

Background

The administration of drugs designed to be given as a single dose rather than as multiple doses has recently been made possible using controlled-release formulations. In this way, drug release can be accomplished over long periods of time, enabling an almost constant level of the drug to be maintained in the bloodstream. Moreover, sustained-release formulations increase the clinical efficacy of drugs.[1] The introduction of drug nanocomposites as sustained-release vehicles has provided a breakthrough in novel drug delivery systems in the field of pharmaceutical technology.[2] Layered double hydroxides (LDH) are widely used for this purpose. Because of their unique properties, such as ease of preparation, low cost, good biocompatibility, low cytotoxicity, and full protection of the drugs loaded,[3–5] LDHs have received considerable attention in the development of sustained-release or controlled-release drug delivery systems.

Correspondence: Mohd Zobir Hussein
Department of Chemistry, Faculty of Science, Universiti Putra Malaysia, Serdang, Selangor, Malaysia 43400
Tel +603 8946 6801
Fax +603 8943 5380
Email mzobir@science.upm.my

Layered double hydroxides are also known as hydrotalcite-like materials and anionic clays. They consist of brucite-like layers containing hydroxides of metal cations M^{2+} and M^{3+}, and possess exchangeable anions, A^{n-} and a variable number of water molecules in the interlayer space. The chemical composition of LDH can be represented by the general formula: $[M^{2+}_{1-x}M^{3+}_{x}(OH)_2]^{x+}(A^{n-})_{x/n}\cdot mH_2O$.[5]

Due to the anionic exchange properties of LDH, many pharmaceutically active compounds, especially those with negative charges or anions, have been intercalated into LDH brucite-like interlayers. As a result of ionic interactions, the intercalated actives are more stable, and usually show sustained release of the cargo molecules, which subsequently results in sustained drug levels. Such a property has been exploited for the controlled-release formulation of drugs such as the anticancer agent, 5-fluorouracil,[6] the anti-inflammatory drug fenbufen,[7] the antihypertensive drugs captopril, lisinopril, enalapril, and ramipril,[8] and cardiovascular drugs, such as pravastatin and fluvastatin.[9]

Perindopril, (2S, 3aS, 7aS)-1-[(2S)-2-[[(2S)-1-ethoxy-1-ox-opentan-2-yl]amino]propanoyl]-2,3,3a,4,5,6,7,7a-octahydroin-dole-2-carboxylic acid is an antihypertensive drug that acts by inhibiting angiotensin-converting enzyme (ACE).[10] Perindopril is a prodrug ester that is converted into the active diacid, perindoprilat, by hydrolysis after administration.[11] It is administered orally in the form of tablets in a 1:1 ratio of perindopril salt with erbumine (tert-butylamine).

Complementary to previous research work,[12,13] and due to the lack of previous studies on the intercalation of perindopril erbumine (PE), we selected this agent as a model drug and intercalated it with Zn/Al-LDH using ion-exchange and coprecipitation techniques. We focused our work on the structure, thermal properties, and slow-release properties of the as-synthesized drug-LDH nanocomposite, with the aim of using the resulting LDH-perindopril nanocomposite as a controlled-release formulation of the active drug, and study the effect of resulting nanocomposites on the angiotensin-converting enzyme.

Materials and methods

Materials

PE ($C_{23}H_{43}N_3O_5$, molecular weight 441.6) was purchased from CCM Duopharma (Berhad, Malaysia) at 99.79% purity and used as received. Other materials, including $Zn(NO_3)_2\cdot 6H_2O$, $Al(NO_3)_3\cdot 9H_2O$, NaOH, ACE, and hippuryl-histidyl-leucine, were purchased from Sigma (St Louis, MO) and used as received. Deionized water was used in all experiments.

Synthesis of Zn/Al-NO_3 LDH

Zn/Al-NO_3 was prepared according to the method described by Miyata[14] with minor modifications. An aqueous solution of 2 mol/L NaOH was added dropwise to a solution (250 mL) containing Zn^{2+} and Al^{3+} (molar ratio of Zn^{2+} to Al^{3+} is 4:1) with vigorous stirring until a pH of 7 was reached; the resulting solution was kept under a nitrogen gas environment. The slurry was aged at 70°C for 18 hours, and then centrifuged and washed with deionized water and dried in an oven at 60°C.

Synthesis of PE-Zn/Al nanocomposite by ion-exchange

PE was intercalated into Zn/Al-NO_3 using the ion-exchange method. An aqueous solution containing 3.54 g (0.008 mol) of PE in 100 mL of decarbonated water was added to 50 mL of an aqueous suspension containing 0.2 g of Zn/Al-NO_3. The mixture was magnetically stirred for 2 hours at room temperature. The resulting material was filtered, washed with water, and finally dried in an oven at 60°C. The product was denoted as PZAE (perindopril intercalated into Zn/Al by ion-exchange).

Synthesis of PE-Zn/Al nanocomposite by coprecipitation

The PE-intercalated Zn/Al-NO_3 was prepared using the coprecipitation method. An aqueous solution containing 2 mol/L NaOH and PE (4.43 g, 0.01 mol) was added dropwise into a solution (250 mL) containing Zn^{2+} and Al^{3+} nitrate (molar ratio of Zn^{2+} to Al^{3+} was 4:1) under a nitrogen atmosphere with vigorous stirring until a pH of 7 was reached. The resulting slurry was kept at 70°C for 18 hours. The aged slurry was then filtered, washed with water, and finally dried in an oven at 60°C. The product was denoted as PZAC (perindopril intercalated into Zn/Al by coprecipitation method).

Controlled-release study

Drug release profiles were determined at room temperature using phosphate-buffered saline at a concentration of 0.01 mol/L and pH 4.8 and 7.4. About 85 mg of each nanocomposite was added to 500 mL of the media. The cumulative amount of PE released into the solution was measured at preset time intervals at λ_{max} = 215 nm using a Perkin Elmer ultraviolet-visible spectrophotometer (model Lambda 35; PerkinElmer, Waltham, MA).

To compare the release rate of perindopril from LDH with that from the physical mixture of PE and Zn/Al-LDH, 0.62 mg of a physical mixture of PE (0.2 mg) and the pristine

LDH (0.42 mg) was used. Release of the active perindopril was determined as described above.

MTT cytotoxicity and in vitro antihypertensive assay

Normal Chang liver cells was seeded at a density of 1×10^4 cells/well into 96-well plates and kept at 5% CO_2 and 37°C for 24 hours. The cell was then treated with PE, PZAE, and PZAC at concentrations of 1.25, 0.625, 0.313, and 0.156 µg/mL. After 24 hours of incubation, cell viability was determined using a colorimetric assay based on the uptake of MTT by viable cells. The MTT-containing medium was removed gently and replaced with dimethylsulfoxide (200 µL/well) to mix the formazan crystals until dissolved. Absorbance at 570 nm and 630 nm (background) was measured with a microtiter plate reader. All experiments were carried out in triplicate. The IC_{50} was generated from the dose-response curves for the cell line.

The in vitro antihypertensive activity of free perindopril and intercalated perindopril in LDH, (PZAE and PZAC) was assayed by measuring their ACE inhibition activity using the method reported by Cushman and Cheung.[15] In vitro ACE inhibition activity was quantified by converting hippuryl-histidyl-leucine to hippuric acid through ACE in the presence of the inhibitor; absorbance was measured at 228 nm. Any reduction in absorbance is proportional to the inhibition exerted by the assayed inhibitor. Perindopril, PZAE, and PZAC (0.5 µg/mL) were preincubated with ACE for 20 minutes in a 25 µL volume in buffer (pH 8.3), then mixed with 10 µL of 3.5 mM hippuryl-histidyl-leucine. The assay mixture was incubated at 37°C for 30, 60, and 90 minutes. The reaction was stopped by adding 50 µL of 3 mol/L HCl. The hippuric acid formed by ACE was extracted with 1 mL of ethyl acetate. The solvent was removed by heat evaporation and re-dissolved in deionized water. The amount of hippuric acid was measured using a fluorescent plate reactor at 228 nm.

Characterization

Powder x-ray diffraction patterns were recorded in the range of 2°C–70°C on a Shimadzu diffractometer, XRD-6000, using CuK_α radiation ($\lambda = 1.5418$ Å) at 30 kV and 30 mA, with a dwell time of 0.5 degrees per minute. Fourier transform infrared (FTIR) spectra of the materials were recorded over the range of 400–4000 cm^{-1} on a Thermo Nicolet Nexus FTIR (model Smart Orbit) with 4 cm^{-1} resolution, using the KBr disc method with a 1% sample in 200 mg of spectroscopic grade potassium bromide, and making the pellets by pressing at 10 tonnes. The chemical composition of the samples was analyzed for zinc and aluminum ions by inductively coupled plasma atomic emission spectrometry using a Perkin-Elmer spectrophotometer (model Optima 2000DV) under standard conditions. For carbon, hydrogen, nitrogen, and sulfur (CHNS) analyses, a CHNS-932 LECO instrument was used. Thermogravimetric and differential thermogravimetric analyses were carried out using a Mettler Toledo instrument with a heating rate of 10°C/minute, in the range of 20°C –1000°C under a nitrogen atmosphere (N_2 flow rate 50 mL/minute). Surface characterization of the material was carried out using the nitrogen gas adsorption-desorption technique at 77 K and a Micromeritics ASAP 2000 instrument. A field emission scanning electron microscope (Nova Nanosem 230 model) was used to determine the surface morphology of the samples. Ultraviolet-visible spectra were measured to determine the optical properties, and a controlled release study was performed using a Perkin Elmer ultraviolet-visible spectrophotometer (Lambda 35).

Results and discussion

Powder X-ray diffraction

The X-ray diffraction patterns of perindopril intercalated into Zn/Al-LDH for the formation of nanocomposites obtained by both the ion-exchange and coprecipitation routes are depicted in Figure 1B and C, respectively. Figure 1A represents the x-ray diffraction pattern of Zn/Al-LDH. As shown in Figure 1A, the 003, 006, and 009 reflections were found for 2θ at about 9.79, 19.72, and 29.74 degrees, respectively. In addition, the two 110 and 113 reflections were found at 60.3 and 61.2 degrees, respectively. The basal spacing value (d_{003}, obtained by averaging the higher order peaks) of the pristine Zn/Al-NO_3 was 9.01 Å, which is consistent with the data in the literature.[16] The characteristic reflections of perindopril shown in Figure 1D were absent from the X-ray diffraction pattern of the product of reaction of PE with Zn/Al-NO_3 LDH, suggesting that perindopril was intercalated into the interlayer galleries of the LDH rather than adsorbed onto the surface. This was confirmed by the shifting of the 003, 006, and 009 diffraction peaks to low 2θ angles at 4.00, 8.31, and 12.5 degrees, respectively, when using the ion-exchange method (Figure 1B), and 4.29, 8.87, and 13.26 degrees, respectively, when using the coprecipitation method (Figure 1C).

The lattice parameters of the Zn/Al-LDH, PZAE, and PZAC samples were calculated from the positions of the maxima due to reflection by planes, ie, 003 for parameter c, where [$c = 1/3(3d_{003} + 6d_{006} + 9d_{009})$, and 110 for parameter a, where ($a = 2d_{110}$)], as shown in Table 1. The reflection line

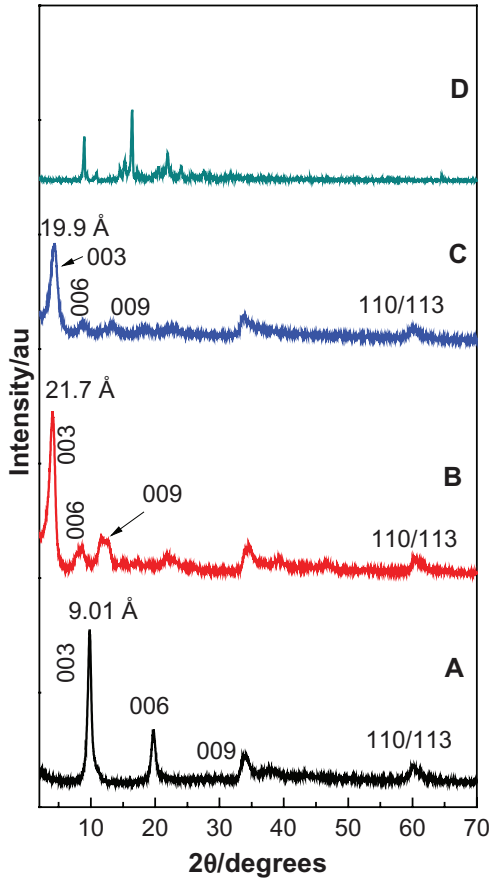

Figure 1 Powder X-ray diffraction patterns for pristine Zn/Al-NO_3 (**A**), the nanocomposite prepared using the ion-exchange method, PZAE (**B**), the coprecipitation method, PZAC (**C**), and perindopril erbumine (**D**).
Abbreviations: Zn, zinc; Al, aluminum; LDH, layered double hydroxide; PZAE, perindopril intercalated into Zn/Al by ion-exchange; PZAC, perindopril intercalated into Zn/Al by coprecipitation method.

of diffraction peak 110 (1.53 Å) for the Zn/Al-LDH sample did not shift after the intercalation process, which indicates that intercalation of perindopril did not change the structure of the layer, but only changed the interlayer spacing.[17]

Molecular structure and spatial orientation of intercalated perindopril

The PE consisted of perindopril (free acid, Figure 2C) combined with erbumine (*tert*-butylamine). This combination incorporates hydrogen bonds (Figure 2A) or involves the transfer of protons from the carboxylic group of perindopril to *tert*-butylamine (Figure 2B). During the intercalation process, the free acid of PE (Figure 2C), which is negatively charged on the carboxylic acid group, is preferentially intercalated into the inorganic interlayers of LDH. Therefore, we presumed that the perindopril anion of PE was intercalated into the inorganic interlayers. We subsequently estimated the dimensions of the perindopril anion and its spatial orientation.

The X-ray diffraction pattern shows that the d-spacing (d_{003}) of the nanocomposites increased to 21.7 (obtained by averaging the higher three order peaks) and 19.9 Å (obtained by averaging the higher five order peaks) for PZAE and PZAC, respectively. Because the thickness of the LDH layer is constant at 4.8 Å,[18] the gallery height of LDH after intercalation can thus be calculated by the d-spacing minus the thickness of the LDH layer; these values were 16.9 Å (21.7–4.80 Å) and 15.1 Å (19.9–4.80 Å) for PZAE and PZAC, respectively. The long and short axes (x-axes and y-axes, respectively) and molecular thickness (z-axis) of perindopril were calculated using Chemoffice software (Cambridge, MA), giving values of 13 Å, 8.4 Å, and 12.6 Å, respectively. The gallery height of PZAE was 16.9 Å, which is much larger than the value of the long axis (13 Å), and slightly similar to double the short axis (16.8 Å). This suggests that the perindopril anions in PZAE were accommodated as an alternate bilayer, as illustrated in Figure 2D. A comparison of the long axis of perindopril (13 Å) with a gallery height of PZAC (15.1 Å) suggests that, in PZAC, perindopril anions were accommodated as a vertical monolayer (along the axis of perindopril) with the presence of water between the perindopril anions and this layer (Figure 2E).[19]

Infrared spectroscopy

The FTIR spectrum of Zn/Al-NO_3 LDH is shown in Figure 3B. The absorption peak at 1384 cm^{-1} is due to nitrate groups. The broad absorption peak at 3452 cm^{-1} can be attributed to stretching of the O-H group, which is contained within the layer. The absorption peak at 1628 cm^{-1} is due to the bending of H_2O,[20] while the absorption at 428 cm^{-1} is due to Zn-Al-OH stretching.[21]

Table 1 Lattice parameters and surface properties of samples

Samples	d_{003} (Å)	d_{110} (Å)	a (Å)	c (Å)	BET surface area (m^2/g)	BJH pore volume (cm^3/g)	BJH pore diameter (Å)
ZnAl-NO_3	9.01	1.53	3.07	27.02	1	0.008	243
PZAE	21.7	1.53	3.07	65.6	2	0.009	135
PZAC	19.9	1.54	3.07	59.8	7	0.025	157

Abbreviations: Zn, zinc; Al, aluminum; NO_3, nitrate; PZAE, perindopril intercalated into Zn/Al by ion-exchange; PZAC, perindopril intercalated into Zn/Al-LDH by coprecipitation method; BJH, Barret-Joyner-Halenda; BET, Brunauer-Emmett-Teller.

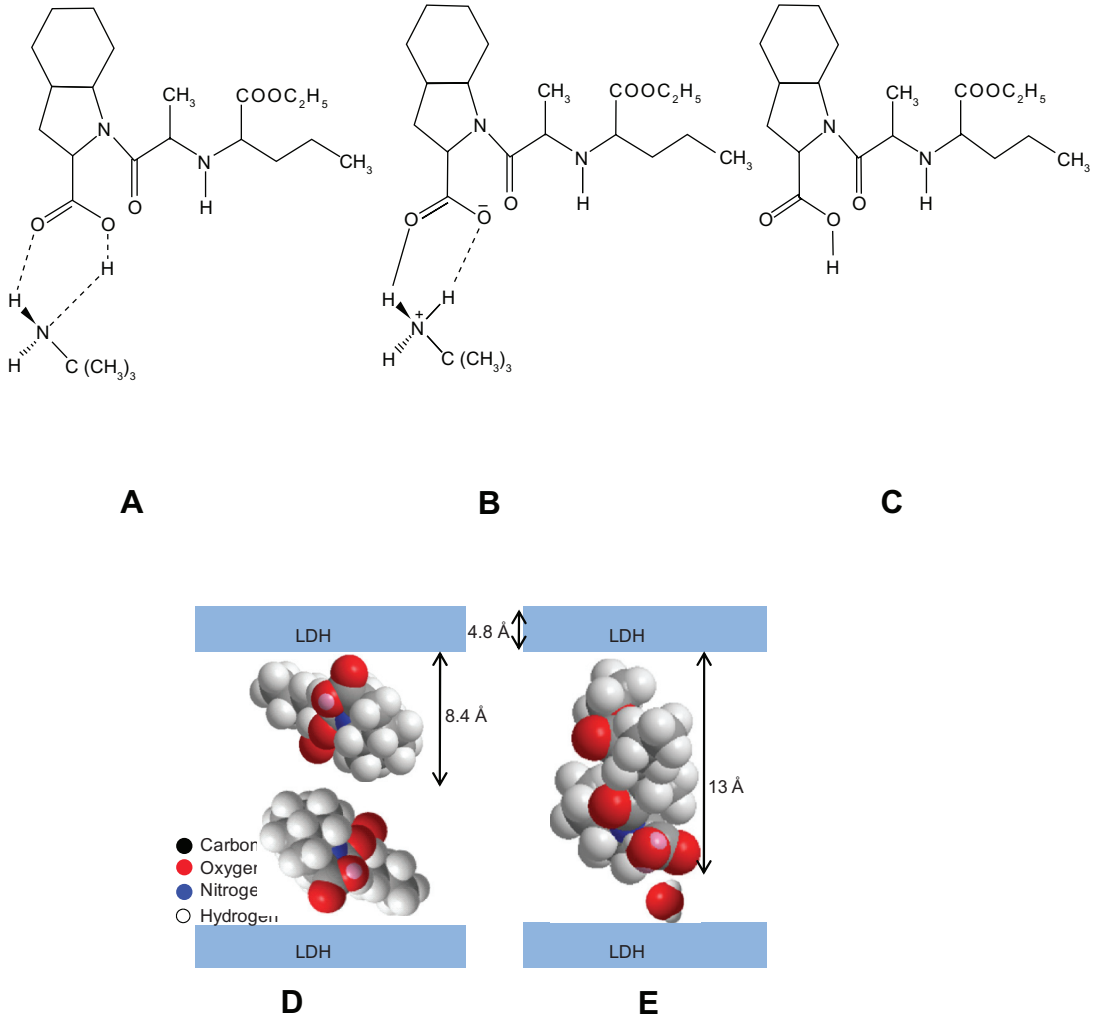

Figure 2 Structure of perindopril erbumine (**A**–**C**) and molecular structural models of perindopril intercalated between the interlayers of LDH (**D** and **E**).
Abbreviation: LDH, layered double hydroxide.

The FTIR spectra of PE (Figure 3A and Table 2) show many intense, sharp absorption peaks that are due to the different functional groups present in the molecules, ie, primary amine, secondary amine, ester, carboxylic acid and methyl groups. Tert-butylamine shows three absorption peaks at 2871 cm^{-1}, which can be attributed to the asymmetric stretching of CH_3,[22] while the peak at 1247 cm^{-1} is due to C_3C–N stretching[22] and 1022 cm^{-1} indicates C–N stretching.[23] The band at 2851 cm^{-1} can be attributed to CH in CH_3–CH–NH and the band at 2929 cm^{-1} is due to CH in NH–CH-propyl. The secondary amine functional group shows a peak at 1154 cm^{-1} which is related to the symmetric stretching of C–N–C.[23] The bands recorded at 1745, 1209, and 1064 cm^{-1} are due to C=O, C–C–O, and O–C–C stretching, respectively, in the ester group.[23] The band at 1731 cm^{-1} is due to the ν(C=O) stretching mode of the carboxylic group, which indicates that PE can exist in a neutral form[24] (Figure 2A). The band at 1291 cm^{-1} is due to C–O stretching in the carboxylic acid group.[25]

The FTIR spectra of the PZAE and PZAC are shown in Figure 4C and D, respectively, and the spectral assignments are shown in Table 2. The nanocomposite spectrum shows the characteristic bands of pure perindopril, which indicate that the perindopril anions are intercalated into the interlayer galleries of LDH. Table 2 shows that some of the bands are slightly shifted in position due to the interaction between the perindopril anion and the interlayers as a result of the intercalation process. The bands recorded at 1732 cm^{-1} and 1729 cm^{-1} for the PZAE and PZAC nanocomposites, respectively, are due to the presence of perindopril in a neutral form adsorbed on the layer or due to an ester group.[26,27] The appearance of new broad peaks at 1613 cm^{-1} for PZAE and 1601 cm^{-1} for PZAC can be assigned to asymmetry stretching vibration of the COO^- group. The shift in COO^- asymmetry

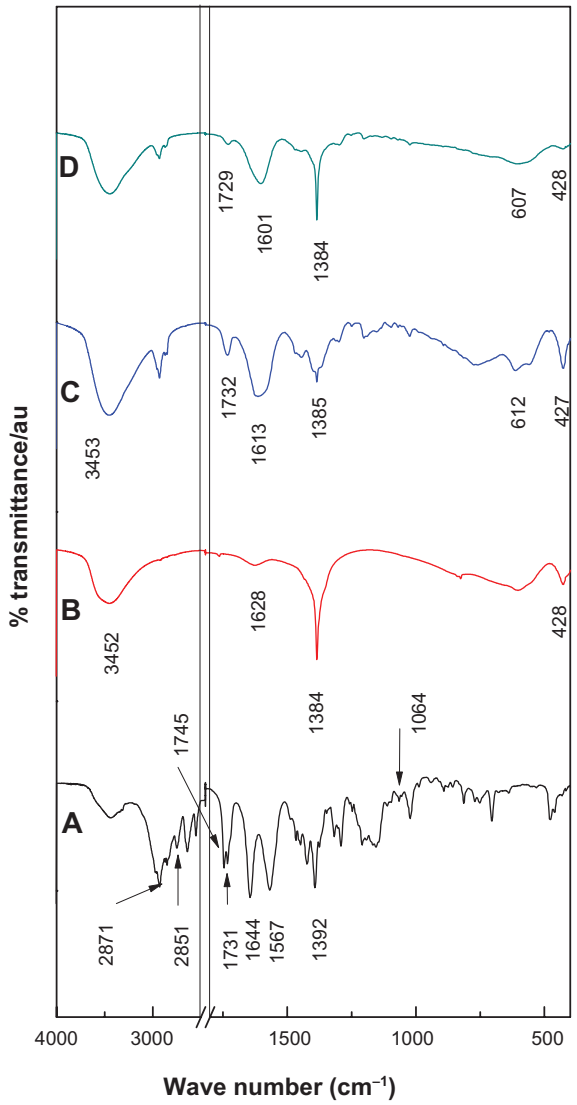

Figure 3 Fourier transform infrared patterns of (**A**) perindopril erbumine, (**B**) Zn/Al-NO_3, (**C**) PZAE, and (**D**) PZAC.
Abbreviations: Zn, zinc; Al, aluminum; LDH, layered double hydroxide; PZAE, perindopril intercalated into Zn/Al by ion-exchange; PZAC, perindopril intercalated into Zn/Al by coprecipitation method.

for the PZAC nanocomposite to a lower wave number compared with PZAE presumably occurred due to the presence of water molecules between the layers, which bind the perindopril molecules and the inorganic interlayer.[28] The band at 1384 cm^{-1} is due to the nitrate anion, which may not be completely removed from the interlayers during the intercalation process, and to the symmetric stretching vibration of the COO^- functional group.[29]

The bands below 600 cm^{-1} are due to metal-oxygen bonds; ν(M-O-M) stretching modes in the layers indicate that the structure of the layers is well maintained.[30,31]

Table 2 Assignment of FTIR absorption bands from PE, PZAE, and PZAC nanocomposites

	PZAE (cm^{-1})	PZAC (cm^{-1})	PE (cm^{-1})
Stretching O–H	3453	3451	–
CH in NH–CH-propyl	2931	2933	2929
C=O in COOH	–	–	1731
Asymmetry COO^-	1613	1601	–
Scissoring CH_2	1468	1469	1466
Asymmetry bending CH_3	1445	1446	1448
NO_3 and symmetry COO^-	1385	1384	–
C–C–O for ester	1202	1202	1209
C–N–C for secondary amine	1152	1132	1154
O–C–C ester	1069	1070	1064

Abbreviations: FTIR, Fourier transform infrared; PE, perindopril erbumine; PZAE, perindopril intercalated into Zn/Al by ion-exchange; PZAC, perindopril intercalated into Zn/Al by coprecipitation method.

Elemental analysis

Elemental analysis was conducted to determine the organic and inorganic composition of PZAE, PZAC, and Zn/Al-NO_3 LDH. As expected, the PZAE and PZAC nanocomposites contained both organic and inorganic constituents. This indicates that intercalation occurred in which perindopril was intercalated into the LDH inorganic interlayers.

Table 3 shows that the Zn^{2+}/Al^{3+} molar ratio in Zn/Al-NO_3 LDH, PZAE, and PZAC is 3.5, 3.45, and 2.6, respectively. As a result of the elemental chemical analysis and thermogravimetric studies, the empirical formula for LDH was determined to be $\left[Zn_{0.78}Al_{0.22}(OH)_2\right](NO_3^-)_{0.22} \cdot 0.31H_2O$. According to the FTIR spectra of PZAC and PZAE, the strong bands at 1384 cm^{-1} and 1385 cm^{-1} are due to the presence of trace amounts of a nitrate group in the interlamellar spacing of LDH. Based on the results of elemental chemical analysis and thermogravimetric studies,

Table 3 Chemical compositions of Zn/Al-NO_3 LDH, PZAE, and PZAC nanocomposites

Samples	Zn%[a]	Al%[a]	C%[b]	N%[b]	C/N	Drug%[b]	Zn^{2+}/Al^{3+}	X
ZnAl-NO_3	38.3	4.5	–	2.5	–	–	3.5	0.22
PZAE	30.6	3.6	23.0	3.0	7.67	37.2	3.48	0.22
PZAC	25.2	3.9	20.7	3.3	6.3	33.4	2.6	0.28

Notes: [a]Calculated upon Industrial Control Products data; [b]calculated upon carbon, hydrogen, nitrogen, and sulfur (CHNS) analysis data.
Abbreviations: Zn, zinc; Al, aluminum; C, carbon; N, nitrogen; NO_3, nitrate; PE, perindopril erbumine; PZAE, perindopril intercalated into Zn/Al by ion-exchange; PZAC, perindopril intercalated into Zn/Al by coprecipitation method.

the empirical formula for PZAC was proposed to be $\left[Zn_{0.72}Al_{0.28}(OH)_2\right](PE^-)_{0.177}(NO_3^-)_{0.103}\cdot 0.91H_2O$. The empirical formula for the PZAE nanocomposite can be given as $\left[Zn_{0.78}Al_{0.22}(OH)_2\right](PE^-)_{0.19}(NO_3^-)_{0.03}\cdot 0.4H_2O$.

Thermal analysis

The thermal behavior of the compounds before and after intercalation of perindopril into LDH was examined using thermogravimetric and differential thermogravimetric analyses. The thermal analysis of Zn/Al-LDH, PZAE, PZAC, and pure PE are shown in Figure 4. For PE (Figure 4A), two main thermal events were clearly observed. The first event, which occurred in the region of 90°C–192°C, was attributed to the melting of perindopril, corresponding to a sharp peak in the differential thermogravimetric curve at 157°C with 24.1% weight loss. This was followed by the second stage at 192°C–312°C, due to the decomposition and subtle combustion of perindopril,[32] corresponding to the strong peak at 276°C and 81.2% weight loss. Figure 4B shows that the thermal decomposition of Zn/Al-LDH progressed through four major stages of weight loss; these occurred at temperature maxima of 100°C, 226°C, 302°C, and 787°C, with weight losses of 5.2%, 15.1%, 10.8%, and 1.2%, respectively. The first stage of weight loss in the range 32°C–152°C is due to the removal of water physisorbed on the external surface of LDH as well as structured water. The second and third stages of weight loss can be attributed to dehydroxylation of the metal hydroxide layers and decomposition of nitrate ions, and were completed at 484°C. The final stage of weight loss is related to the formation of spinel.[33]

Following the intercalation process, the thermal decomposition characteristics of the resulting product were significantly different from those of the precursors. The thermogravimetric analysis curves for PZAE and PZAC showed four stages of weight loss. For PZAE (Figure 4C), the first weight loss of 4.2% was attributed to the elimination of surface water or physically adsorbed water and interlayer water at 63°C.[34] The second and third weight losses were attributed to dehydroxylation of the layers and combustion of the perindopril at 199°C and 346°C, respectively. The

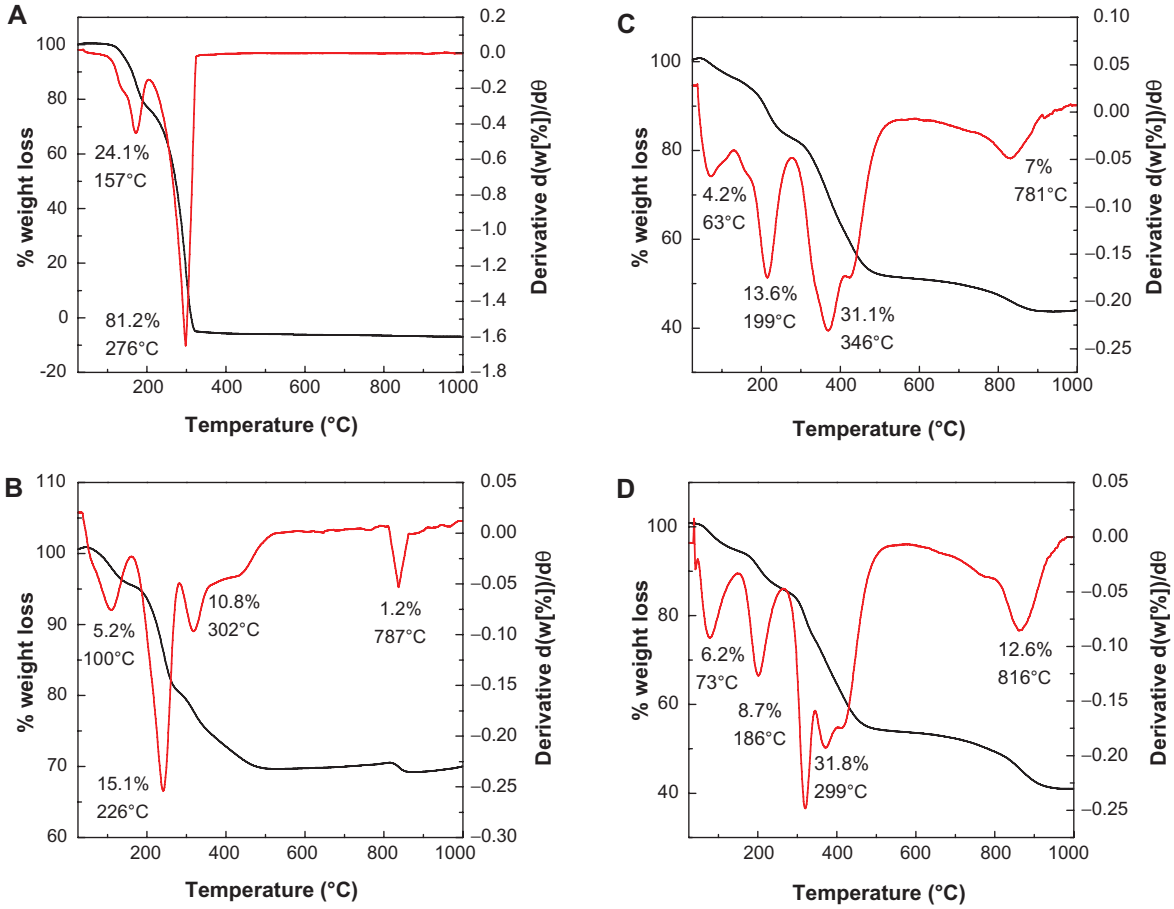

Figure 4 Thermogravimetric and differential thermogravimetric analyses of perindopril (**A**), Zn/Al-NO_3 (**B**), PZAE (**C**), and PZAC (**D**)
Abbreviations: Zn, zinc; Al, aluminum; NO_3, nitrate; PZAE, perindopril intercalated into Zn/Al by ion-exchange; PZAC, perindopril intercalated into Zn/Al by coprecipitation method.

second and third stages usually overlapped.[35] The fourth step with 7% weight loss at 781°C was due to the formation of $ZnAl_2O_4$.

The thermal decomposition characteristics of PZAC were similar to those of PZAE. Three weight losses at 73°C, 186°C, and 299°C were associated with the removal of surface-adsorbed water, interlayer water, and dehydroxylation of the layer, as well as decomposition of perindopril, accompanied by 6.15%, 8.69%, and 31.8% weight loss, respectively (Figure 4D). Decomposition of perindopril in the PZAE and PZAC nanocomposites occurred at 346°C and 299°C, respectively, which is higher than that for free perindopril (276°C). This suggests that the thermal stability of perindopril in nanocomposites was clearly enhanced due to the intercalation process, which involves electrostatic attraction between the negatively charged functional group of perindopril and the positively charged brucite-like layers of LDH.

Surface properties

Figure 5A shows the nitrogen adsorption-desorption isotherms for Zn/Al-NO_3, PZAE, and PZAC. All adsorption isotherms were Type IV according to the International Union of Pure and Applied Chemistry classification, indicating a mesoporous-type material.[36] Adsorption increased slowly at low relative pressure in the range of 0.0–0.8, followed by rapid adsorption at relative pressures >0.8, reaching an optimum at more than 7.1, 6.9, and 18.9 cm^3/g at standard temperature and pressure for Zn/Al-NO_3, PZAE, and PZAC, respectively. The desorption branch of the hysteresis loop in PZAE and PZAC was wider than that of Zn/Al-NO_3, indicating a difference in pore texture. This was due to modification of the pores as a result of the expansion of basal spacing due to the formation of the new nanocomposites.[21]

Table 1 shows the Brunauer-Emmett-Teller (BET)-specific surface area of Zn/Al-NO_3 LDH and the nanocomposites, PZAE and PZAC. As shown in Table 1, the BET-specific surface area of the resulting nanocomposites was higher than that of LDH. The BET surface area increased from 1 m^2/g for Zn/Al-NO_3 to 2 m^2/g for PZAE and 7 m^2/g for PZAC.

Figure 5B shows the Barret-Joyner-Halenda (BJH) desorption pore size distribution for Zn/Al-NO_3, PZAE, and PZAC. As shown, a single-peaked pore size distribution was observed for Zn/Al-NO_3, centered around 178 Å. On the other hand, PZAE and PZAC showed single peaks at 185 Å and 109 Å, respectively. The average pore volume and pore diameter shown by BJH desorption are given in Table 1. The BJH average pore diameters for Zn/Al-NO_3, PZAE and PZAC were 243 Å, 135 Å, and 157 Å, respectively; the BJH pore volumes for the same samples were 0.008, 0.009, and 0.025 cm^3/g, respectively.

The surface morphology of Zn/Al-NO_3 LDH, PZAE, and PZAC is illustrated in Figure 6. All samples showed typical non-uniform irregular agglomerates of compact and non-porous plate-like structures, similar to the morphology of nanocomposites discussed in the literature.[37] PZAC had a smoother surface morphology than Zn/Al-NO_3 LDH and PZAE.

Sustained-release study

The cumulative release profiles of perindopril from PZAE and PZAC, and its physical mixture, PE, with Zn/Al-LDH in solution at pH 7.4 and 4.8, are shown in Figure 7.

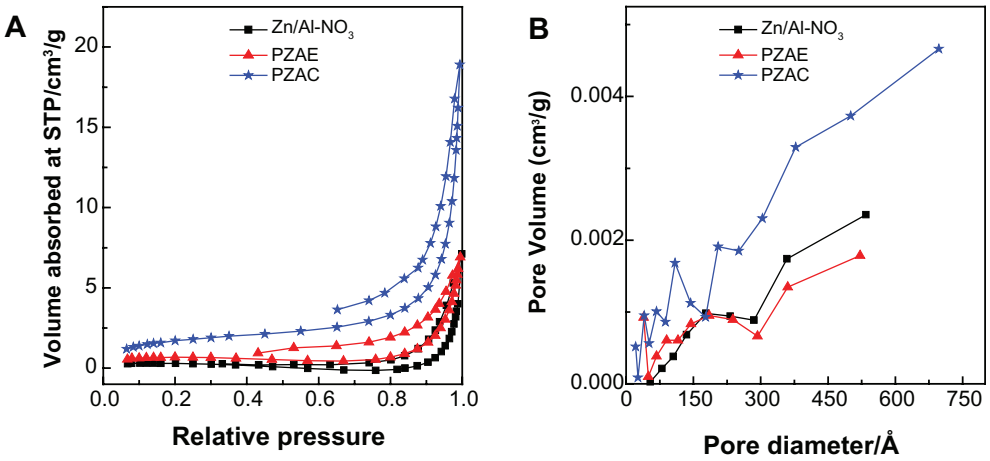

Figure 5 Adsorption-desorption isotherms (**A**) and BJH pore size distributions (**B**) for Zn/Al-NO_3, PZAE, and PZAC.
Abbreviations: BJH, Barret-Joyner-Halenda; Zn, zinc; Al, aluminum; NO_3, nitrate; PZAE, perindopril intercalated into Zn/Al by ion-exchange; PZAC, perindopril intercalated into Zn/Al by coprecipitation method; STP, standard temperature pressure.

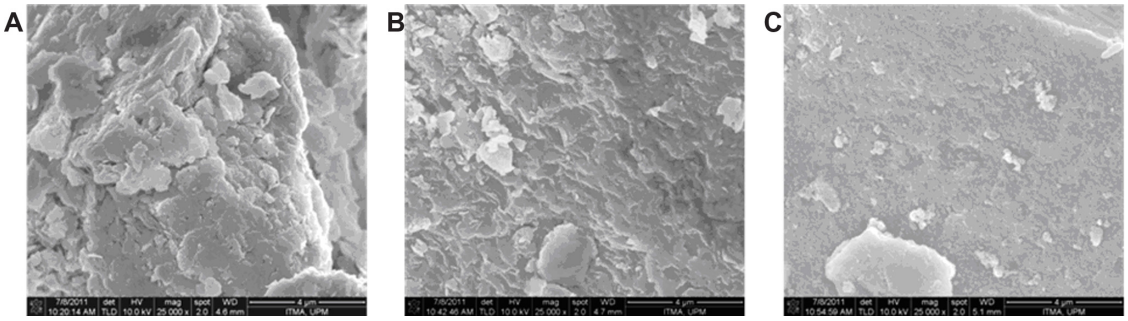

Figure 6 Field emission scanning electron micrographs of ZnAl-NO_3 (**A**), PZAE (**B**), and PZAC (**C**) at 25,000×.
Abbreviations: Zn, zinc; Al, aluminum; NO_3, nitrate; PZAE, perindopril intercalated into ZnAl by ion-exchange; PZAC, perindopril intercalated into ZnAl by coprecipitation method.

The physical mixture showed no sustained-release effects in both solutions at pH 7.4 and 4.8, with the total PE content released immediately. At pH 7.4 and 4.8, the release rate within the first 12 minutes reached 87% and 97%, respectively. However, the perindopril-intercalated LDH nanocomposite gradually released perindopril anions over time, both at pH 7.4 and 4.8. At pH 4.8 (Figure 7I [B and D]), the first aliquot contained a large number of perindopril anions due to the "burst effect",[38] together with the release of perindopril anions adsorbed onto the outer surface of LDH. Subsequently (in acid media at pH 4.8), the LDH particles were destroyed and the intercalated perindopril drug anions were released. The destruction of the layers increased the acidity (pH) of the solution and increased the rate of perindopril release in this medium. Therefore, release was faster at pH 4.8 than at pH 7.4. When the drug–LDH dissolution process reached equilibrium, 87% was released in 1100 minutes and 1020 minutes for PZAE and PZAC, respectively (Figure 7II [B and D]).

At pH 7.4 (Figure 7I [A and C]), the release of perindopril was rapid within the first 200 and 300 minutes, which can be attributed to the release of perindopril anions adsorbed on the outer surface of LDH as well as intercalated perindopril. Subsequently, however, the release of perindopril became much slower and sustained compared with the solution at pH 4.8, with a total release equilibrium of 83% in 1263 minutes for PZAC and 70% in 1000 minutes for PZAE (Figure 7II [A and C]). This sustained-release process may be attributed to the ion-exchange process between the perindopril anions and the anions in the buffer solution.[39,40] The release profile of perindopril from PZAE and PZAC shown in Figure 8 is similar to that of other drugs from the host.[6,8,41–43]

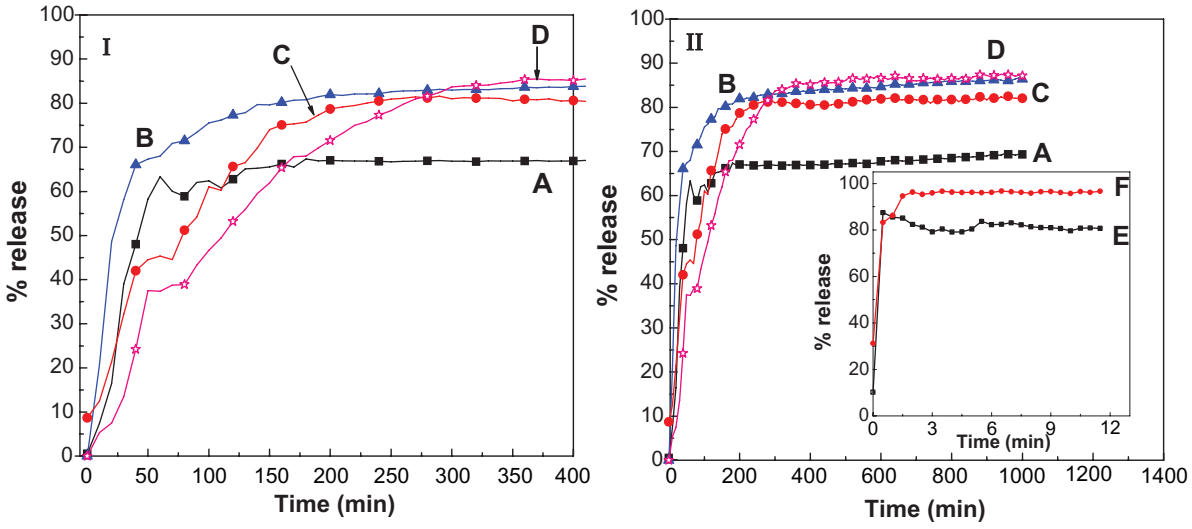

Figure 7 (**I**) Release profiles of perindopril from the PZAE sample at pH 7.4 (**A**) and pH 4.8 (**B**), and from the PZAC sample at pH 7.4 (**C**) and pH 4.8 (**D**) up to 400 minutes, (**II**) release profiles of perindopril up to 1260 minutes. Inset shows the release profiles of perindopril from its physical mixture of perindopril with Zn/Al-NO_3 at pH 7.4 (**E**) and pH 4.8 (**F**).
Abbreviations: Zn, zinc; Al, aluminum; NO_3, nitrate; PZAE, perindopril intercalated into Zn/Al by ion-exchange; PZAC, perindopril intercalated into Zn/Al by coprecipitation method.

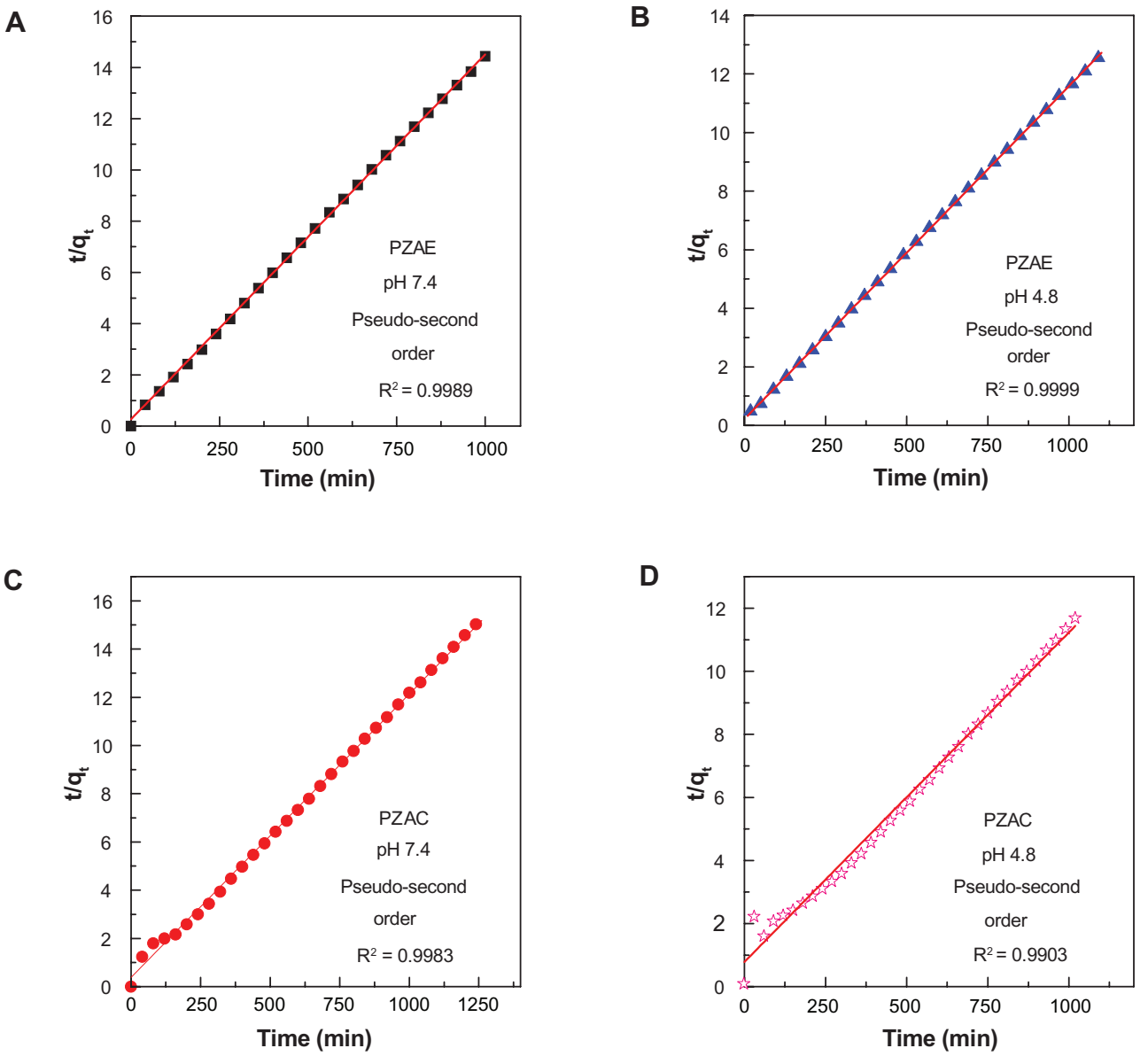

Figure 8 Fitting the perindopril release data from PZAE samples (**A** and **B**) and from PZAC samples (**C** and **D**) at pH 4.8 and 7.4.
Abbreviations: PZAE, perindopril intercalated into Zn/Al by ion-exchange; PZAC, perindopril intercalated into Zn/Al by coprecipitation method.

Additionally, at pH 7.4, the duration of release of perindopril, which was arranged as a monolayer in the PZAC sample, was much longer than that of PZAE, which was arranged in a bilayer fashion (Figure 2D and E). It is possible that the perindopril anions that were arranged in a monolayer fashion in the interlayer showed weaker repulsive forces and a stronger affinity for the LDH interlayers. Thus, these structures may have been more difficult to destroy compared with the anions arranged in bilayers.

To gain more insight into the mechanism of release of perindopril from the nanocomposites, we used three types of kinetic models to fit the release data:

a. The pseudo-first order model,[41] which expresses release of perindopril from LDH; here the dissolution rate depends on the amount of perindopril in the nanocomposite and can be expressed as:

$$\ln (q_e - q_t) = \ln q_e - k_1 t \quad (1)$$

b. The pseudo-second order kinetic equation,[41] which is represented in the form:

$$t/q_t = 1/h + t/q_e \quad (2)$$

where q_e and q_t are the equilibrium release amount and the release amount at any time (t), respectively, and $h = k_2 q_e^2$.

Table 4 Correlation coefficient (R^2), rate constants (k), and half-time ($t_{1/2}$) obtained by fitting the perindopril release data from PZAE and PZAC nanocomposites into solutions at pH 4.8 and 7.4

Samples	pH	Saturation release (%)	R^2			Pseudo-second order	
			Pseudo-first order	Pseudo-second order	Parabolic diffusion model	Rate constant, K (mg/min) × 10^{-4}	$t_{1/2}$ (minutes)
PZAE	7.4	70	0.7026	0.9989	0.3846	7.4	18.9
PZAE	4.8	87	0.8417	0.9999	0.4530	5.7	19.3
PZAC	7.4	83	0.6035	0.9983	0.5120	3.8	31.6
PZAC	4.8	87	0.7842	0.9903	0.6956	1.3	77

Abbreviations: PZAE, perindopril intercalated into Zn/Al by ion-exchange; PZAC, perindopril intercalated into Zn/Al by coprecipitation method.

c. The parabolic diffusion model,[44] which can be expressed as:

$$(1 - M_t/M_o)/t = k_d t^{-0.5} + a \quad (3)$$

where a is constant and k_d is the overall diffusion constant for release. M_o and M_t are the amount of perindopril between the layers at release time 0 and t, respectively.

The data on perindopril release from the nanocomposites into the solutions were fitted into the above mentioned equations. The corresponding linear coefficient (R^2) was evaluated, is summarized in Table 4, and is plotted in Figure 8. As shown, the pseudo-second order model was the most satisfactory for describing the release kinetics of perindopril from the nanocomposites, similar to previous studies reported in the literature.[41] Figure 8 shows the plots of t/q_t against t for the release of perindopril at pH 4.8 and 7.4. As shown, straight lines were obtained. For the release of perindopril at pH 4.8, the correlation coefficient values were 0.9999 and 0.9903 for PZAE and PZAC, respectively, whereas the correlation coefficients at pH 7.4 were 0.9989 and 0.9983 for PZAE and PZAC, respectively.

Table 4 shows the pseudo-second order rate constant for the release of perindopril from PZAE and PZAC. At pH 4.8, this was 5.7×10^{-4} and 1.3×10^{-4} mg/minute, respectively. At 7.4, the values were 7.4×10^{-4} and 3.8×10^{-4} mg/minute, respectively.

MTT cytotoxicity and in vitro antihypertensive activity

Figure 9 show the effect of PE, PZAE, and PZAC on viability, using Chang cells at various concentrations of 0.156, 0.313, 0.625, and 1.25 µg/mL and with 24-hour incubation times. As shown in Figure 9, PE did not have a cytotoxic effect on the viability of these cells. Interestingly, the PZAE and PZAC also had no toxic effect on the Chang cells at a concentration up to 1.25 µg/mL. These results are consistent

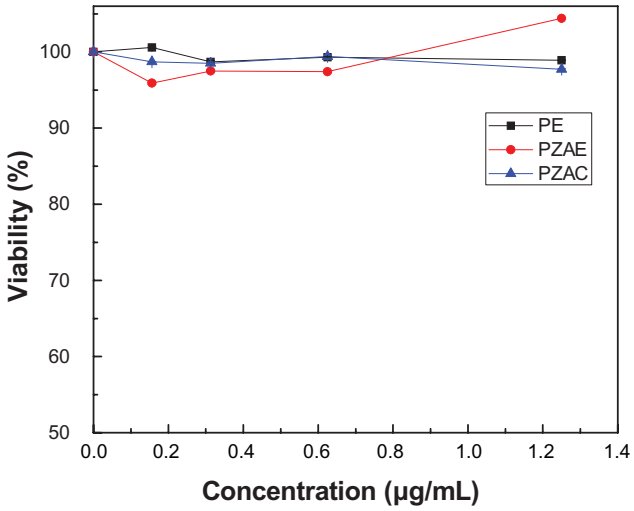

Figure 9 MTT assays of normal Chang liver cells after 24 hours of treatment with perindopril erbumine, PZAE, and PZAC.
Abbreviations: PZAE, perindopril intercalated into Zn/Al by ion-exchange; PZAC, perindopril intercalated into Zn/Al by coprecipitation method.

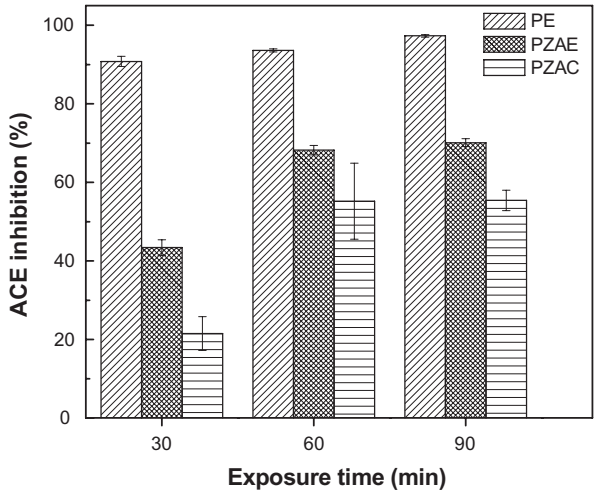

Figure 10 Angiotensin-converting enzyme inhibition (%) for free perindopril and perindopril intercalated into PZAE and PZAC after 30, 60, and 90 minutes of exposure time.
Abbreviations: PE, perindopril erbumine; PZAE, perindopril intercalated into Zn/Al by ion-exchange; PZAC, perindopril intercalated into Zn/Al by coprecipitation method.

Table 5 Angiotensin-converting enzyme activity for PE, PZAE, and PZAC with different exposure times

Exposure time (minutes)	PE	PZAE	PZAC
30	90.8	43.4	21.5
60	93.6	68.2	55.2
90	97.3	70.1	55.4

Abbreviations: PE, perindopril erbumine; PZAE, perindopril intercalated into Zn/Al by ion-exchange; PZAC, perindopril intercalated into Zn/Al by coprecipitation method.

with those of a study reported by Posati et al who showed that cytotoxicity is apparently selective for human cervical adenocarcinoma epithelial (HeLa) cells, because there is no significant cytotoxicity towards non-malignant Madin-Darby canine kidney cells.[45]

Several other investigations have demonstrated the antihypertensive potential of PE.[46–48] Figure 10 and Table 5 show the first report of free Zn/Al layered double hydroxide and PE intercalated into Zn/Al, with ACE inhibition activity. The ACE inhibition activity of perindopril in PZAE and PZAC nanocomposites was determined in vitro by monitoring the transformation from a substrate hippuryl-histidyl-leucine to the product hippuric acid. Of the two formulations, the PZAE showed the most potent ACE inhibition activity. That may be attributable to the high level of PE release from the PZAE nanocomposite when compared with PZAC. However, the ACE inhibition activity of both formulations was time-dependent. Zn/Al layered double hydroxide did not show that inhibition. Following incubation of ACE with 0.5 μg/mL of PZAE, approximately 43% and 68% decreases in ACE activity were observed at 30 and 60 minutes of incubation, respectively, as compared with the untreated cells. Under these same conditions, incubation of ACE with PZAC (0.5 μg/mL) resulted in 21% and 55% decreases in ACE activity at these same time points, respectively. Table 5 shows slightly decreases in ACE activity with 0.5 μg/mL of PZAE and PZAC for 90 minutes as compared with that for 60 minutes.

Conclusion

This work shows that intercalation of perindopril, an antihypertensive drug, into Zn/Al-LDH can be accomplished using two methods, namely ion-exchange and coprecipitation. The basal spacing of the nanocomposites was expanded to 21.7 Å and 19.9 Å when using ion-exchange and coprecipitation, respectively. The results suggest that the perindopril molecules were arranged as a monolayer within the interlayers when using the coprecipitation method and as a bilayer when using the ion-exchange method. As a result of the intercalation process, the thermal stability and sustained release of the intercalated perindopril were considerably enhanced compared with its free counterpart. The duration of release of perindopril from the nanocomposite prepared by the coprecipitation method was much longer than that of perindopril prepared by the ion-exchange method at pH 7.4. It is possible that the intercalated guest molecules, arranged in a monolayer fashion within the interlayers, have a weaker repulsive force and stronger affinity towards the LDH interlayers. The release of perindopril from the nanocomposite was found to be governed by pseudo-second order kinetics. An in vitro antihypertensive assay showed that the intercalation process has similar effectiveness on the antihypertensive properties of perindopril.

Acknowledgment

We would like to thank the Ministry of Higher Education of Malaysia for funding the project under grant 05-03-10-1035 RUGS (Vot 9199644). The author is grateful to Universiti Putra Malaysia for International Graduate Research Fellowship (IGRF).

Disclosure

The authors declare that they have no competing interests in this work.

References

1. Rathbone MJ, Hadgraft J, Roberts MS. *Modified-Release Drug Delivery Technology*. *Volume 126*. New York, NY: Marcel Dekker; 2003.
2. Neeraj V, Taehong M, Rhul M, et al. Development of PEGylated PLGA nanoparticles for controlled and sustained drug delivery in cystic fibrosis. *J Nanobiotechnology*. 2010;8(22):1–18.
3. Choi S-J, Choy J-H. Layered double hydroxide nanoparticles as target-specific delivery carriers: uptake mechanism and toxicity. *Nanomedicine*. 2011;6(5):803–814.
4. Shi W, Wei M, Jin L, Li C. Calcined layered double hydroxides as a "biomolecular vessel" for bromelain: immobilization, storage and release. *J Mol Catal B Enzym*. 2007;47(1–2):58–65.
5. Williams GR, O'Hare D. Towards understanding, control and application of layered double hydroxide chemistry. *J Mater Chem*. 2006;16(30):3065–3074.
6. Wang Z, Wang E, Gao L, Xu L. Synthesis and properties of Mg_2 Al layered double hydroxides containing 5-fluorouracil. *J Solid State Chem*. 2005;178(3):736–741.
7. Li B, He J, Gevans D, Duan X. Inorganic layered double hydroxides as a drug delivery system – intercalation and in vitro release of fenbufen. *Appl Clay Sci*. 2004;27(3–4):199–207.
8. Xia SJ, Ni ZM, Xu Q, Hu BX, Hu J. Layered double hydroxides as supports for intercalation and sustained release of antihypertensive drugs. *J Solid State Chem*. 2008;181(10):2610–2619.
9. Panda HS, Srivastava R, Bahadur D. In-vitro release kinetics and stability of anticardiovascular drugs – intercalated layered double hydroxide nanohybrids. *J Phys Chem B*. 2009;113(45):15090–15100.
10. Opie LH. *Angiotensin-Converting Enzyme Inhibitors: Scientific Basis for Clinical Use*. *Volume 2*. 2nd ed. New York, NY: Wiley-Liss New York; 1994.

11. Pascard C, Guilhem J, Vincent M, Remond G, Portevin B, Laubie M. Configuration and preferential solid-state conformations of perindoprilat (S-9780). Comparison with the crystal structures of other ACE inhibitors and conclusions related to structure-activity relationships. *J Med Chem*. 1991;34(2):663–669.
12. Hussein MZ, Al Ali SH, Zainal Z, Hakim MN. Development of antiproliferative nanohybrid compound with controlled release property using ellagic acid as the active agent. *Int J Nanomedicine*. 2011;6: 1373–1383.
13. Al Ali SHH, Al-Qubaisi M, Hussein MZ, Zainal Z, Hakim MN. Preparation of hippurate-zinc layered hydroxide nanohybrid and its synergistic effect with tamoxifen on HepG2 cell lines. *Int J Nanomedicine*. 2011; 6:3099–3111.
14. Miyata S. Hydrotalcites in relation to composition. *Clays Clay Miner*. 1980;28(1):50–56.
15. Cushman DW, Cheung HS. Spectrophotometric assay and properties of the angiotensin-converting enzyme of rabbit lung. *Biochemical Pharmacology*. 1971;20(7):1637–1648.
16. Tang P, Xu X, Lin Y, Li D. Enhancement of the thermo- and photostability of an anionic dye by intercalation in a zinc-aluminum layered double hydroxide host. *Ind Eng Chem Res*. 2008;47(8):2478–2483.
17. Kong X, Shi S, Han J, Zhu F, Wei M, Duan X. Preparation of glycy-L-tyrosine intercalated layered double hydroxide film and its in vitro release behavior. *Chem Eng J*. 2010;157(2–3):598–604.
18. Cavani F, Trifiro F, Vaccari A. Hydrotalcite-type anionic clays: Preparation, properties and applications. *Catal Today*. 1991;11(2): 173–301.
19. Meyn M, Beneke K, Lagaly G. Anion-exchange reactions of layered double hydroxides. *Inorg Chem*. 1990;29(26):5201–5207.
20. Carbajal Arizaga GG, Wypych F, Castillon Barraza F, Contreras Lopez OE. Reversible intercalation of ammonia molecules into a layered double hydroxide structure without exchanging nitrate counter-ions. *J Solid State Chem*. 2010;183(10):2324–2328.
21. Hussein MZ, Hwa TK. Synthesis and properties of layered organic-inorganic hybrid material: Zn-Al layered double hydroxide-dioctyl sulfosuccinate nanocomposite. *J Nanopart Res*. 2000;2(3):293–298.
22. Kipkemboi PK, Kiprono PC, Sanga JJ. Vibrational spectra of *t*-butyl alcohol, *t*-butylamine and *t*-butyl alcohol+ *t*-butylamine binary liquid mixtures. *B Chem Soc Ethiopia*. 2003;17(2):211–218.
23. Smith BC. *Infrared Spectral Interpretation: A Systematic Approach*. Boca Raton, FL: CRC; 1999.
24. Milan R. Molecular structure and stability of perindopril erbumine and perindopril l-arginine complexes. *Eur J Med Chem*. 2009;44(1): 101–108.
25. Tronto J, Reis MJD, Silverio F, Balbo VR, Marchetti JM, Valim JB. In vitro release of citrate anions intercalated in magnesium aluminium layered double hydroxides. *J Phys Chem Solids*. 2004;65(2–3): 475–480.
26. Kempa TJ, Barton ZM, Cunliffe AV. Mechanism of the thermal degradation of prepolymeric poly(3-nitratomethyl-3-methyloxetane). *Polymer*. 1999;40(1):65–93.
27. Kir'yalov N, Amirova G. Triterpene acids from the roots of Meristotropis triphylla Fisch. et Mey. *Chem Nat Compd*. 1965;1(5):243–245.
28. Morzyk-Ociepa B, Michalska D, Pietraszko A. Structures and vibrational spectra of indole carboxylic acids. Part I. Indole-2-carboxylic acid. *J Mol Struct*. 2004;688(1–3):79–86.
29. Yuan Q, Wei M, Evans DG, Duan X. Preparation and investigation of thermolysis of L-aspartic acid-intercalated layered double hydroxide. *J Phys Chem B*. 2004;108(33):12381–12387.
30. Rives V. *Layered Double Hydroxides: Present and Future*. New York, NY: Nova Science Publishing Inc; 2001.
31. Kloprogge JT, Frost RL. Fourier transform infrared and Raman spectroscopic study of the local structure of Mg-, Ni-, and Co-hydrotalcites. *J Solid State Chem*. 1999;146(2):506–515.
32. Macêdo RO, Gomes do Nascimento T, Soares Arago CF, Barreto Gomes AP. Application of thermal analysis in the characterization of anti-hypertensive drugs. *J Therm Anal Calorim*. 2000;59(3):657–661.
33. Cheng X, Huang X, Wang X, Sun D. Influence of calcination on the adsorptive removal of phosphate by Zn-Al layered double hydroxides from excess sludge liquor. *J Hazard Mater*. 2010;177(1–3):516–523.
34. Ajat M, Mohd M, Yusoff K, Hussein MZ. Synthesis of glutamate-zinc-aluminium-layered double hydroxide nanobiocomposites and cell viability study. *Curr Nanosci*. 2008;4(4):391–396.
35. Vicente R. Characterisation of layered double hydroxides and their decomposition products. *Mater Chem Phys*. 2002;75(1–3):19–25.
36. Pierotti RA, Rouquerol J. Reporting physisorption data for gas/solid systems with special reference to the determination of surface area and porosity. *Pure Appl Chem*. 1985;57(4):603–619.
37. Raki L, Beaudoin JJ, Mitchell L. Layered double hydroxide-like materials: nanocomposites for use in concrete. *Cem Concr Res*. 2004; 34(9):1717–1724.
38. Huang X, Brazel CS. On the importance and mechanisms of burst release in matrix-controlled drug delivery systems. *J Control Release*. 2001;73(2–3):121–136.
39. Bin Hussein MZ, Zainal Z, Yahaya AH, Foo DWV. Controlled release of a plant growth regulator,[alpha]-naphthaleneacetate from the lamella of Zn-Al-layered double hydroxide nanocomposite. *J Control Release*. 2002;82(2–3):417–427.
40. Ambrogi V, Fardella G, Grandolini G, Perioli L, Tiralti MC. Intercalation compounds of hydrotalcite-like anionic clays with anti-inflammatory agents, II: uptake of diclofenac for a controlled release formulation. *AAPS Pharm Sci Tech*. 2002;3(3):77–82.
41. Dong L, Yan L, Hou W-G, Liu S-J. Synthesis and release behavior of composites of camptothecin and layered double hydroxide. *J Solid State Chem*. 2010;183(8):1811–1816.
42. Hou WG, Jin ZL. Synthesis and characterization of naproxen intercalated Zn-Al layered double hydroxides. *Colloid Polym Sci*. 2007; 285(13):1449–1454.
43. Wei M, Pu M, Guo J, et al. Intercalation of L-dopa into layered double hydroxides: enhancement of both chemical and stereochemical stabilities of a drug through host-guest interactions. *Chem Mater*. 2008; 20(16):5169–5180.
44. Kodama T, Harada Y, Ueda M, Shimizu K-I, Shuto K, Komarneni S. Selective exchange and fixation of strontium ions with ultrafine Na-4-mica. *Langmuir*. 2001;17(16):4881–4886.
45. Posati T, Bellezza F, Tarpani L, et al. Selective internalization of ZnAl-HTlc nanoparticles in normal and tumor cells. A study of their potential use in cellular delivery. *Appl Clay Sci*. 2012;55(0):62–69.
46. Chrysant SG, McDonald RH, Wright JT, Barden PL, Weiss RJ. Perindopril as monotherapy in hypertension: a multicenter comparison of two dosing regimens. *Clin Pharmacol Ther*. 1993;53(4):479–484.
47. Rahman N, Anwar N, Kashif M. Optimized and validated initial-rate method for the determination of perindopril erbumine in tablets. *Chem Pharm Bull*. 2006;54(1):33–36.
48. Sica DA. Dosage considerations with perindopril for systemic hypertension. *Am J Cardiol*. 2001;88(7):13–18.